FRACTAL ANALYSIS OF THE ENVIRONMENTAL RADIOACTIVITY:A REVIEW

Vasile CUCULEANU[1,2], Mărgărit PAVELESCU[2]

Abstract *This paper provides a review of literature related to the assessment of the fractal characteristics of the time series of environmental radioactivity using rescaled range(R/S) analysis, as well as the box counting method. The R/S analysis allows to estimate the Hurst exponent and the fractal dimension of a time series of data that is studied. The Hurst exponent can classify a given time series in terms of whether it is a random, a persistent, or an anti-persistent process. The analysed physical data are the natural and artificial radioactivity concentrations from the environmental components (atmosphere, soil, water).*

1. Introduction

A great number of physical systems tend to present similar behaviours on different scales of measured data. Benoit Mandelbrot has introduced the term fractal and corresponding concepts of fractal geometry and fractal dimension to indicate objects whose complex geometry cannot be characterized by an integral dimension [1,2]. The word fractal comes from Latin and means irregular. The more complex definition of fractals, given by Mandelbrot, is based on the concept of self-similarity: a fractal is a shape made by parts similar to the whole in some way [2]. This definition entails scale invariance of the appearance of parts of a whole. A set is strictly self-similar if it can be expressed as a union of sets, each of which is geometrically similar to the full set.[3].The word fractal was introduced from the necessity of describing from dimensional point of view the variable shapes of the geometrical figures /functions and the natural elements (the coastlines of waters, the mountains), which could not be described by the Euclidean geometry. The fractal dimension contains information about geometrical irregularities of fractal objects over multiple scales. The fractal dimension of a curve, for instance, will lie between 1 and 2, depending on how much area it fills. The fractal dimension can then be used to compare the complexity of two curves [4].

The fractal dimension of an attractor measures to what extent the dynamics fills the embedding phase space and provides a lower bound for the number of independent variables necessary to model the time dependence of the physical system [5, 39].

[1]Faculty of Physics, University of Bucharest, 077125 Bucharest- Magurele, P.O. Box MG-11, Romania.
[2]Academy of Romanian Scientists, 54 Splaiul Independentei, RO-050094, Bucharest, Romania.

The purpose of the present paper is to analyze the published papers dealing with the fractal and multifractal characteristics of the environmental radioactivity in order to make evident the performances of this approach for highlighting the real dynamics of the concentrations of radionuclides in the respective environment.

2. Elements of fractal theory

In order to calculate the fractal dimension of a time series it is used the Hurts exponent which is estimated by making use of the rescaled range analysis.

2.1 Rescaled range analysis

The rescaled range analysis was introduced by Hurst [6] being considered a new statistical method. Let C (t) be a time dependent observable specific to a physical dynamic system.

In this case one may consider C(i) as being the specific activity(or concentration) of a radionuclide in a component of environmental radioactivity during any time interval *i*, in which the sampling takes place.

One assumes that the time series of radionuclide concentration contain N values, $\{C(i)\}_{i=1,N}$, corresponding to N equal sampling intervals.

The mean concentration on a number $\boldsymbol{\tau}$ of sampling intervals is:

$$\langle C \rangle_{\tau} = \frac{1}{\tau} \sum_{i=1}^{\tau} C(i) \qquad (1)$$

Let $X(t,\boldsymbol{\tau})$ be the accumulation function that represents the summation of the differences between the concentration $C(i)$ and the average $\langle C \rangle_{\tau}$:

$$X(t,\tau) = \sum_{i=1}^{t} \{C(i) - \langle C \rangle_{\tau}\}, \; t = 1,2,\ldots,\tau \qquad (2)$$

The range of differences between the maximum and the minimum of the accumulation function for the different τ, is denoted by R:

$$R(\tau) = \max_{1 \le t \le \tau} X(t,\tau) - \min_{1 \le t \le \tau} X(t,\tau) \qquad (3)$$

The range R depends on the value of $\boldsymbol{\tau}$ and is expected to increase with increasing $\boldsymbol{\tau}$. To investigate different phenomena, Hurst used the dimensionless ratio R/S, where S is the standard deviation, i.e., the square root of variance. The expression for S is:

$$S = \left[\frac{1}{\tau}\sum_{i=1}^{\tau}\{C(i) - \langle C\rangle_{\tau}\}^2\right]^{1/2} \qquad (4)$$

Hurst mentioned that the rescaled range function *R/S* for many natural records in time, is well described by the following empirical relation [7]:

$$\frac{R}{S} \cong \alpha\tau^{H} \qquad (5)$$

for all scales or time lags $\boldsymbol{\tau}$**.** In this relation α is a constant of proportionality. The coefficient *H* calculated from the fit of *ln*(R/S) against *ln*$\boldsymbol{\tau}$ is named the Hurst exponent.

The time series analysed by Hurst obviously show that for many natural phenomena $H>1/2$, while for records generated by statistically independent processes with finite variances $H = 1/2$. When $1/2 < H < 1$ the record indicates a persistent behaviour; in this case if the time series for some time in the past has a positive increment - i.e., an increase- then it also has on the average an increase in the future. Therefore, an increasing trend in the past implies an increasing trend in the future for the process with H>1/2, and, in addition, this is applicable for all relevant time scales, including the longest. Inversely, a decreasing trend in the past implies on the average a continued decrease in the future. When H <1/2 the time series has an anti-persistent time dependence, i.e., has an increasing trend in the past implies a decreasing trend in the future, and a decreasing trend in the past points out a possible increase in the future. If a time series of a physical observable is specific to a diffusion process, the value H>1/2 characterizes the environments where intense diffusion processes dominated by turbulent diffusion occur. In order to justify these ideas regarding the H coefficient, the normalized correlation function is considered between previous and future values [7]:

$$2^{2H-1} - 1 \qquad (6)$$

Thus, if H <1/2 the correlation function is negative and there is anti-persistence; if $H = 1/2$ there is no correlation what is specific to an independent random process; if H>1/2 the correlation is positive and the respective time series exhibits persistence.

2.2 Fractal dimension

A fractal is by definition a set for which the Hausdorff-Besicovitch dimension strictly exceeds the topological dimension [1]. A set of points making up a line in the Euclidean space has a topopogical dimension 1 and the Hausdorff-Besicovitch dimension 1. Fractal is a geometric shape that is self-similar and has a fractional

dimension, unlike the Euclidean geometric figures that have integer dimensions. The Hausdorff dimension or fractal dimension is considered the measure of the irregularity of a curve representing a time series. To measure the 'size' of a set of points, the embedding space (line, surface, volume) is divided into geometric units (segments, squares, cubes) of side *l*. Considering the number of units necessary to cover the set of points, *N(l)* , a measure of the set size can be obtained :

$$M_d = N(l) \cdot l^d \qquad (7)$$

where d=1,2,3 for line, surface, and volume respectively.

If the set of points makes up a curve of length L_0 its measure for unit segments of length *l* is:

$$(M_1)_{curve} = N(l) \cdot l = L_0 \cdot l^0 \text{ , since } N(l) = L_0 / l \qquad (8)$$

The measure of the 'area' of this curve is:

$$(M_2)_{curve} = N(l) \cdot l^2 = L_0 \cdot l^1 \underset{l \to 0}{\to} 0 \qquad (9)$$

Therefore, as it was normally, the 'area' of a curve is zero. Let us consider a set of points defining a surface of area A_0. The normal measure of the respective set of points is:

$$(M_2)_{area} = N(l) \cdot l^2 = A_0 \cdot l^0 \qquad (10)$$

since $N(l) = A_0 / l^2$

If a 'length' is associated with this surface, one obtains the following result :

$$(M_1)_{area} = N(l) \cdot l = A_0 \cdot l^1 \underset{l \to 0}{\to} \infty \qquad (11)$$

Generally, as $l \to 0$, the measure M_d is either zero, constant, or infinity depending on the choice of *d* , named dimension of measure. The Hausdorff-Besicovitch or fractal dimension D_B of an experimental data set is the critical dimension for which the *d*-measure M_d of the set varies from zero to infinity (when $l \to 0$):

$$M_d = N(l) \cdot l^d \to \{0,\ d > D_B \qquad (12)$$

$$M_d = N(l) \cdot l^d \to \{\infty,\ d < D_B \qquad (13)$$

When the value of M_d is finite(not zero or infinity) for $d = D_B$, the number of coverings *N(l)* has the following dependence on *l* and D_B :

$$N(l) \propto l^{-DB} \text{ for } l \to 0 \qquad (14)$$

By plotting ln *N(l)* as function of ln *l* the fractal dimension D_B can be determined. The expression of the measure for a curve shows that for a line $D_B = 1$, and the

expression the measure for an area shows that for a plane $D_B = 2$. When the fractal dimension is non-integer, the set of points that generated the respective D_B has fractal properties. These properties are specific to physical systems that may be described by non-linear mechanism and many variables which strongly interact in such way that they become unpredictable. Such physical systems generate the chaotic time series. It has been shown that in non-linear systems that exhibit deterministic chaos, the multi-dimensional dynamic information can be recovered from a time series of measurements of a single variable [8].This approach allows for the recovery of information from all degrees of freedom which are coupled to an observable. Thus, the strange attractor of a chaotic dynamical system may be extracted from a time series of experimental data of a single physical quantity. As is obvious from Fig. 1. the radon time series makes up a self-affine set of points, this curve reproducing itself in some sense under the affine transformation [9].

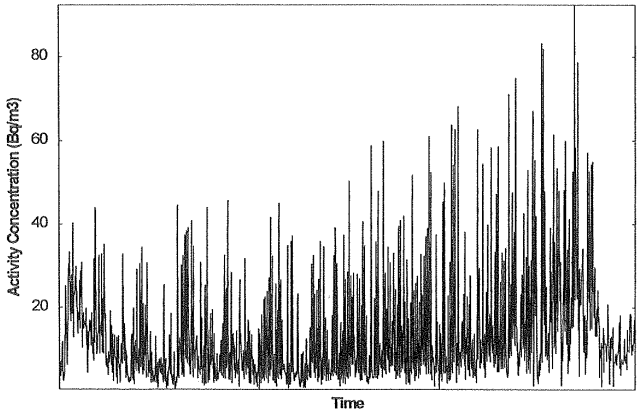

Figure 1. Radon time series,1-y period (1990)[5]

The fractal dimension for self-affine data is given by:

$$D_H = 2 - H \qquad (15)$$

3. Environmental radioactivity

The environmental radioactivity refers to the radioactivity of atmosphere (air), lithosphere (soil and subsoil), hydrosphere (surface and underground water) and vegetation

3.1. Radioactivity

The property of nuclei to spontaneously emit without external intervention α, β particles and γ radiation is called radioactivity. The process is known as radioactive decay, and the respective element is also called radionuclide or radioisotope. If the elements naturally exist, radioactivity is named natural. When

radionuclides occur as a result of human action (nuclear reactions in laboratories, nuclear explosions, controlled emissions from nuclear installations or other types), the radioactivity is called artificial.

In the current language, particles α and β are called α and β radiation, although they are not of electromagnetic nature.

The α particle consists of helium nuclei (^4_2He). Following the α decay of a ^A_ZX nucleus, it passes into a nucleus $^{A-4}_{Z-2}Y$ (A is the mass number and Z atomic number of the elements X and Y) and a α particle with well-determined energy is emitted:

$$^A_ZX \rightarrow {}^{A-4}_{Z-2}Y + {}^4_2\alpha$$

The α particles emitted by natural radionuclides have energies ranging from 3-6 MeV

(1 MeV = $1.6 \cdot 10^{-13}$ J), a 3^{-10}cm path in the air and is strongly ionizing the gases it flows through.

The β particles consist of electrons (β^-) and positrons (β^+). In a β^- decay, a neutron in the nucleus turns into a proton, an electron and an antineutrino ($n \rightarrow p + e^- + \nu$□), resulting in an increase of the atomic number with a unit:

$$^A_ZX \rightarrow {}^A_{Z+1}Y + e^- + \tilde{\nu}$$

The positron is a particle with identical physical characteristics to the electron but with a positive charge. During the β^+ decay, a proton in the nucleus turns into a neutron, a positron and a neutrino ($p \rightarrow n + e^+ + \nu$), and the resulting nucleus has a smaller atomic number with one unit:

$$^A_ZX \rightarrow {}^A_{Z-1}Y + e^+ + \nu$$

The β particles have a lower ionization power than the α particles, but a higher penetration power. For example, the β particles with energies of about 1 MeV pass several meters in air or 2 ÷ 3 mm in aluminum.

The γ radiation is of electromagnetic nature, has very little wavelength ($10^{-9} \div 10^{-12}$ cm), is much more penetrating than the α or β particles and can easily pass a few meters in the air or a few tens of centimeters in lead.

3.1.1. Physical quantities and units used in the environmental radioactivity

In the domain of the environmental radioactivity are used both quantities and usual units of radioactivity as well as quantities and specific units.

•**Half-life** ($T_{1/2}$) - the time interval after which half of the initial number of nuclei disintegrate is known as the *half-life*. The units currently used are: second, minute, hour, day, year.

•**Radioactive constant** (λ) - The probability that a radionuclide will decay in the time unit is called the *radioactive constant* or the *disintegration constant.* The *mean life* or *lifetime* (τ) of a radioactive nucleus is $\tau = 1/\lambda$.

•**Activity** (Λ)- Let N be the number of nuclei from a radioactive element at a time t in a sample. The number of nuclei that disintegrate in the unit of time, $\Lambda = \lambda N$, is called the *activity* of the sample. The unit of measure for Λ is 1 Becquerel (Bq); 1Bq = 1disintegration / second. A tolerated unit is 1 Curie(Ci):1Ci = $3.7 \cdot 10^{10}$ disintegrations/sec = $3.7 \cdot 10^{10}$ Bq. There are radioactive nuclei that can disintegrate in several ways. If the competitive disintegration modes of a radionuclide have disintegration probabilities λ_1, λ_2, λ_3, ... the total probability of disintegration will be $\lambda = \Sigma\ \lambda i$. Partial activity of a sample containing N nuclei, which refers to some disintegration mode, *i*, is defined by $\Lambda_i = \lambda i\ N$. The total activity is: $\Lambda = \Sigma\ \Lambda_i$.

•**Specific activity** (Λs)

Let us consider an environment (air, water, soil, vegetation) in which radioactive substances are present. *Specific activity* is defined as the number of radioactive disintegrations per unit time and unit of volume or mass. The unit of measure is Bq/m3 for air, Bq/l for water, Bq/kg for soil and vegetation. A quantity related to the specific activity is the concentration of nuclei (C) which represents the number of nuclei of a given species per unit volume or mass: $\Lambda s = \lambda\ C$. For the tritium activity, a 1UT unit (a tritium unit) is used which represents a concentration of one tritium atom at 10^{18} hydrogen atoms. Expressed as activity 1UT is equivalent to 6.6 disintegrations / minute / liter of water.

•**Dosimetric quantities**

The absorbed dose is the physical quantity that measures the intensity of radiation interaction with matter. The absorbed dose is defined as the energy delivered by the ionizing radiation to the mass unit of the substance with which it interacts. The unit of measurement of the absorbed dose is 1 *Gray* (Gy) which corresponds to an energy of 1 J given to 1 kg of the mass of the substance: 1 Gy = 1 J / kg. Also used is the tolerated unit rad: 1 rad = 0.01 J/kg = 0.01 Gy

The equivalent dose is defined as the dose absorbed in a tissue subjected to any radiation that produces the same biological effect as an absorbed dose corresponding to a standard radiation (X radiation of 200KeV).The unit of measurement in SI also refers to the energy of 1J given to the mass unit by the incident radiation, but to distinguish the two dosimetric quantities (the absorbed dose refers to any substance and the equivalent dose to the biological tissue) the name of *sievert* (Sv) was introduced. There is also the tolerated unit rem: 1 rem = 10^{-2} Sv.

The effective dose is the equivalent dose to irradiation of a tissue that produces the same effect as uniform body irradiation. For example, the average annual effective dose due to the atmospheric radon and descendants is about 1 mSv.

3.2. Natural radioactivity

The phenomenon of natural radioactivity refers to the radionuclides naturally found on Earth. This radioactivity was discovered by Becquerel at the end of the nineteenth century (1896). Natural radionuclides are essential constituents of the Earth since its formation. Four billion and a half years later, the interior of the Earth is still heated by the disintegration of the long-lived isotopes of uranium, thorium and potassium. Natural radioactivity is both terrestrial and extraterrestrial origin. Approximately 340 nuclides have been found in nature, of which about 70 are radioactive and are mainly heavy elements. All elements with an atomic number greater than 80 have radioactive isotopes and all isotopes with an atomic number greater than 83 are radioactive [10, 11].

3.2.1. Primordial and secondary radionuclides

Natural radionuclides are contained in the atmosphere, the lithosphere, the hydrosphere and the biosphere. At the beginning of the history of the universe, matter contained a large number of radioactive isotopes, but over the time all isotopes with a shorter half-life ($T_{1/2}$) have disappeared, in the present existing in nature only those having the half-life comparable to the age of universe. Radioisotopes with a half-life less than 10^8 years are no longer detectable, since after more than 30 such periods they have completely disappeared, unlike the radionuclides with $T_{1/2}>10^{10}$ years, which disintegrated quite a bit until the present. Isotopes with a sufficiently long $T_{1/2}$ that allowed them to survive the time interval from formation of Earth up to the present are known as primordial radionuclides, and those resulting from their disintegration are called secondary radionuclides. Natural radionuclides may appear singly or in the decay chains of the uranium series (origin element ^{238}U), the thorium series(origin element ^{232}Th), and actinium series (origin element ^{235}U). All three radioactive series (or families) are found in the Earth's crust.

Uranium

Natural uranium contains three isotopes: ^{234}U (0.0058%), ^{235}U (0.71%) and ^{238}U (99.28%). ^{235}U is the basic element used to produce energy in nuclear reactors. It can be considered that in an act of fission one releases energy of about 200 MeV. Uranium is found in all components of the earth: in the atmosphere the concentration varies between 1.3 and 17 $\mu Bq/m^3$, in rocks and soil between 0.03 and 120 ppm, and in the oceans, ^{235}U has a concentration of $1.5\cdot10^{-8}$g/L and ^{238}U of $2\cdot10^{-6}$g/L. The radioactive series of ^{238}U and ^{235}U are presented in Tables 1 and 2 [11].

Table 1. Uranium Series

Nuclide	Historical name	Half-life	Major radiations
^{238}U	Uraniu I	$4,47 \cdot 10^9$ y	α, < 1% γ
^{234}Th	Uraniu X_1	24,1 z	β, γ
^{234m}Pa	Uraniu X_2	1,17 m	β, < 1% γ
^{234}Pa	Uraniu Z	21,8 m	β, γ
^{234}U	Uraniu II	244.500 y	α, < 1% γ
^{230}Th	Ioniu	$7,7 \cdot 10^4$ y	α, < 1% γ
^{226}Ra	Radiu	1600 y	α, γ
^{222}Rn	Radon	3,8 d	α, < 1% γ
^{218}Po	Radiu A	3,05 m	α, < 1% γ
⇆			
^{214}Pb (99,98%)	Radiu B	26,8 m	β, γ
^{218}At (0,02%)	Astatiniu	2 s	α, γ
^{214}Bi	Radiu C	19,9 m	β, γ
⇆			
^{214}Po (99,98%)	Radiu C'	164 μs	α, < 1% γ
^{210}Tl (0,02%)	Radiu C"	1,3 m	β, γ
^{210}Pb	Radium D	22,3 y	β, γ
^{210}Bi	Radiu E	5,01 d	β
⇆			
^{210}Po (~100%)	Radiu F	138,4 d	α, < 1% γ
^{206}Tl (0,00013%)	Radiu E"	4,20 m	β, < 1% γ
^{206}Pb	Radiu G	Stable	

Table 2. Actinium Series

Nuclide	Historical name	Half-life	Major radiations
^{235}U	Actinouraniu	$7,038 \cdot 10^8$ y	α, γ
^{231}Th	Uraniu Y	25,5 h	β, γ
^{234}Pa	Protoactiniu	$2,276 \cdot 10^4$ y	α, γ
^{227}Ac	Actiniu	21,77 y	β, < 1% γ
⇆			
^{227}Th (98,62%)	Radioactiniu	18,72 y	α, γ
^{223}Fr (1,38%)	Actiniu K	21,8 m	β, γ
^{223}Ra	Actiniu X	11,43 d	α, γ
^{219}Rn	Actinon	3,96 s	α, γ
^{215}Po	Actiniu A	1,78 ms	α, < 1% γ
⇆			
^{211}Pb (~100%)	Actiniu B	36,1 m	β, γ
^{215}At(0,00023%)	Astatiniu	~ 0,1 ms	α, < 1% γ
^{211}Bi	Actiniu C	2,14 m	α, γ
⇆			
^{211}Po (0,273%)	Actiniu C'	0,516 s	α, γ
^{207}Tl (99,73%)	Actiniu C"	4,77 m	β, < 1% γ
^{207}Pb	Actiniu D	Stable	

Radium - 226

Nuclide ^{226}Ra disintegrates by the emission of α particles with $T_{1/2}$ = 1622 years and passes to ^{222}Ra, a radioactive isotope ($T_{1/2}$ = 3.8 days) of radon noble gas. ^{226}Ra is present in all types of rocks and soils. Volcanic rocks contain higher amounts than limestone or sedimentation (sandstone). The mean soil concentration is $2.7 \cdot 10^{-2}$ Bq/g [10]. The concentration of ^{226}Ra in the surface water (the first 400 m) of the oceans is of the order of $3.7 \cdot 10^{-6}$ Bq/L [10]. In drinking water the mean concentration is $1.5 \cdot 10^{-3}$ Bq/L [10].

Thorium

The thorium is a primordial element found in the rocks, with the largest amount being present in volcanic rocks, between 8-33 ppm, and the smallest in calcareous rocks, ~ 1 ppm. Sand (sandy rock) contains about 6 ppm. Because of its low solubility it is present in biological tissues in insignificant amounts. For example, the ^{232}Th content in human bones varies between 0.006-0.01 μg/g of ash (bones) [10]. The significant biological effects of ^{232}Th are due to its descendants. In the thorium series, the ^{228}Ra, the β-particle emitter, has the longest half-life, 5.8 years. The direct descendant of ^{228}Ra is ^{228}Th which, through a series of α disintegrations, passes into ^{220}Rn, a radon noble gas isotope, also known as a thoron. The radioactive series of ^{232}Th is presented in Table 3 [11].

Table 3. Thorium Series

Nuclide		Historical name	Half-life	Major radiations
^{232}Th		Thoriu	$1,4 \cdot 10^{10}$ y	α, < 1% γ
^{228}Ra		Mesothoriu I	5,75 y	β, < 1% γ
^{228}Ac		Mesothoriu II	6,13 h	β, γ
^{238}Th		Radiothoriu	1,91 h	α, γ
^{224}Ra		Thoriu X	3,66 d	α, γ
^{220}Rn		Toron	55,6 s	α, < 1% γ
^{216}Po		Thoriu A	0,15 s	α, < 1% γ
^{212}Pb		Thoriu B	10,64 h	β, γ
^{212}Bi		Thoriu C	60,55 m	α, γ
^{212}Po (64%)		Thoriu C'	0,305 μs	α
	^{208}Tl (36%)	Thoriu C''	3,07 m	β, γ
^{208}Pb		Thoriu D	Stable	

A fourth series, that of the neptunium, having ^{241}Pu origin, has disappeared long ago since the ^{241}Pu has a half-life of 14 years and the other elements in the series also have a relatively short $T_{1/2}$ [10]. The only surviving element in this series is ^{209}Bi, with $T_{1/2}$ extremely high (~ $2 \cdot 10^{17}$ years), which makes it almost stable.

Natural radionuclides which are yielded in the atmosphere as a result of the interaction between cosmic radiation and the constituents of the atmosphere are called cosmogenic radionuclides (e.g.: ^{7}Be, ^{14}C, $_{3}H$).

According to their origin, natural or as a result of human action, radionuclides are divided into natural and artificial. Some radionuclides (e.g.: ^{114}Nd) that are in the terrestrial crust and ocean, appear as fission products of ^{235}U, ^{238}U, ^{232}Th, caused by neutrons that appear either in cosmic radiation, either following reactions (α, n) with light elements, or as a result of fission of other nuclei.Because the natural radionuclide (and artificial, around nuclear objectives) are found in all environmental components (air, soil, water, vegetation), are also found in food and, therefore, are present in the human body, causing internal irradiation, and those from the environment, external irradiation.

Radon (^{222}Rn), thoron (^{220}Rn) and their daughters

Radon and thoron are radioactive noble gases. As shown, ^{222}Rn appears in the uranium series having ^{226}Ra as precursor and ^{220}Rn in the thorium series and has ^{224}Ra as precursor. From the Earth's crust the two gases enter the atmosphere through molecular diffusion and convection (Figure 2).The radon exhalation rate has an average value of $2 \cdot 10^{-2}$ Bq m^{-2} s^{-1}(or 10^{4}nuclei $m^{-2}s^{-1}$); the corresponding thoron values are about 1 Bq m^{-2} s^{-1} (or 10^{2} nuclei m^{-2} s^{-1}).The emanation of the two noble gases in the soil depends on the type of soil, its physical conditions, such as moisture, frost, snow, as well as weather conditions such as air pressure and temperature, wind. The exhalation of radon in seas and oceans is about two orders of magnitude smaller than in the soil, which is also found in concentrations in the air above the ocean and the land. Once in the atmosphere, the two radioactive gases are subjected to physical processes specific to the atmosphere (diffusion, transport) and disintegrate, giving rise to daughters. After a time of 10-100 s from the occurrence, daughters attach themselves to aerosols (with dimensions between 10^{-2} - 1 μm) existing in the atmosphere. Following the α disintegration, the attached atoms may be detached from aerosols as a result of the recoil due to emission of the α particles.

Radon decay products are divided into two groups:

-short-lived daughters, ^{218}Pa (RaA), ^{214}Pb (RaB), ^{214}Bi (RaC) and ^{214}Po (RaC ') having a half-life less than 30 min;

-long-lived daughters, ^{210}Pb (RaD, $T_{1/2}$ = 22.3 years), ^{210}Bi (RaE, $T_{1/2}$ = 5 days) and ^{210}P (RaF, $T_{1/2}$ = 138.4 days).

The thoron has no long-life daughters. The most important nuclide in its disintegration chain is ^{212}Pb with $T_{1/2}$ = 10.6h. The disappearance of daughters from atmosphere is due to radioactive disintegration and to the specific removal

processes from the atmosphere of the aerosols to which they were attached: wet deposition and dry deposition. Daughters are also involved in the air diffusion and transport processes. The time variation of the atmospheric concentration of ^{220}Rn and ^{222}Rn depends on the variation in the exhalation rate and the vertical and horizontal dispersion of the two gases. The maximum emanation from soil is usually observed during summer and the minimum in winter. However, the turbulent vertical mixture is more intense in spring and summer, which results in a decrease in the concentration of radon and thoron in the surface layer of the atmosphere. Autumn and winter the vertical turbulent exchange is weaker and thermal inversions are more frequent. The effect of decreasing the intensity of the turbulent mixture being dominant leads to the relative increase of the concentration in the autumn and winter seasons, even if the exhalation in the soil decreases. Thus there is a *seasonal variation* of radon and thoron concentration with a minimum during spring and summer and a maximum during autumn and winter (except in cases where there is a snow layer - the concentration of the thoron being negatively influenced by its thickness). The daily variation of the concentration is characterized by a minimum at noon and a maximum during the night [12]. Measurements carried out in different geographical areas show that the average radon concentration is between 1-10 Bq / m^3 in continental areas and between 0.002-0.2 Bq / m^3 in island and above ocean areas [13].

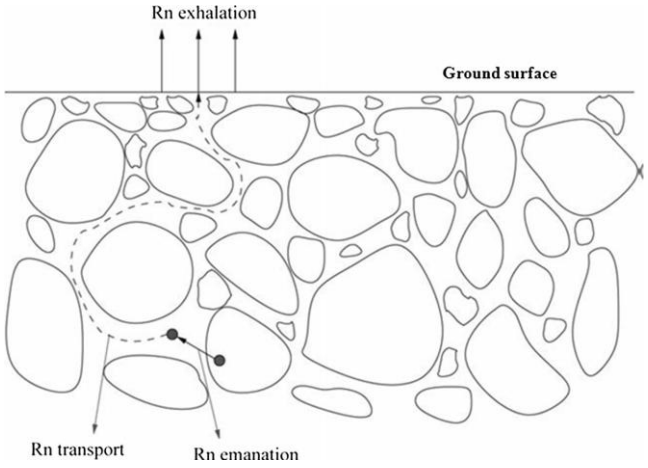

Fig. 2. Release of the radon atoms from mineral grains to the atmosphere[16].

There are measurements that indicate values of radon concentration around 100 Bq/m^3 at ground level under conditions of thermal inversion during the night, when the turbulent mixture is very weak [13, 14]. The studies of thoron and daughters are more limited than those of radon. Thoron measurements indicate that concentration values are dependent on exhalation, weather conditions, and height with respect to ground. The thoron concentration at 1 m height may vary between 1-200 Bq m^3 depending on the soil type and the intensity of the turbulent

mixture in the layer near the soil, and the daughters may have concentrations in the range of 0.01-1 Bq/m^3 [14]. In Romania, measurements performed over a period of 9 years (1980-1988) led to monthly average values of 1-9 Bq/m^3 for daughters of radon and 0.001-0.5 Bq/m^3 for daughters of the thoron [15]. Since ^{222}Rn is in radioactive equilibrium with short-lived daughters, it can be admitted that the specific activity of radon is comparable to that of the daughters.

3.2.2 Cosmogenic radionuclides

A number of radionuclides existing on the Earth's surface and in the atmosphere were produced by interactions between the high energy particles of cosmic radiation and the nuclei of the atmosphere's constituents, mainly, nitrogen, oxygen and argon. Direct radiation to the upper boundary of the atmosphere, which derives from the cosmic space, is known as primary cosmic radiation and consists of protons (91.5%), α particles (7.8%) and nuclei of lithium, beryllium, boron, carbon, nitrogen, oxygen, iron. These radiation are of galactic nature, and a certain fraction of solar origin. The solar component becomes very important in the maximum periods of solar activity with the 11-year cycle. After interacting with the nuclei of atmospheric constituents, cosmic radiation produces mainly electrons, photons, neutrons, protons and mesons (known as secondary cosmic radiation).The resultant neutrons with very high energies in turn produce spallation (or fragmentary) nuclear reactions by which a nucleus of an atmospheric element is "broken" giving rise to a new element and several nucleons. The time variation of the rate of cosmogenic radionuclide production can be due to two different effects: variations in cosmic radiation intensity and variations of the Earth's magnetic field. During periods of weak magnetic field, the production of ^{14}C as well as the other cosmogenic nuclides had maximum values. The main cosmogenic radionuclides are: ^{14}C, also known as radiocarbon, ^{3}H, ^{7}Be.

Radiocarbon, ^{14}C

^{14}C is predominantly produced by the neutron capture reaction from secondary cosmic radiation by atmospheric nitrogen nuclei:

$$^{14}N + n \rightarrow {}^{14}C + p$$

Radiocarbon disintegrates β^- with a half-life of ~ 5730 years and passes into ^{14}N.

The rate of production of ^{14}C by the neutron flux from the secondary cosmic radiation is 1.6 $atoms/cm^2/s$ [10]. Neutrons that produce capture reactions on nitrogen nuclei may also come from atmospheric nuclear explosions. These sources, together with fossil carbon combustion, have increased the ^{14}C concentration at the planetary level.

Radiological impact of ^{14}C is due to inhalation and ingestion of food and water. The biological half-life is about 10 days.

Tritium , ^{3}H

Tritium is generated by the reaction with nitrogen nuclei with relatively large energies:

$$^{14}N + n \rightarrow {}^{3}H + {}^{14}C$$

Tritium disintegrates β^-, with $T_{1/2} = 12.3$ years and passes into helium:

$$^{3}H \rightarrow {}^{3}He + \beta^- (0{,}0181MeV)$$

As in the case of the radiocarbon, tritium concentrations in the atmosphere were higher during atmospheric nuclear explosions. After the cessation of nuclear experiences, tritium began to decline, which is also confirmed by the waters from melting glaciers from Alps. The radiological impact is determined by ingested water, inhalation and absorption through the skin. For a standard human, the biological half-life is 12 days. Tritium, like radiocarbon, is a radionuclide whose origin can be both natural and artificial (when appearing from the fission of ^{235}U and ^{239}Pu).

Beryllium-7, ^{7}Be

^{7}Be is produced by the spallation reaction of ^{14}N and ^{16}O:

$$^{14}N + n \rightarrow {}^{7}Be + 3p + 5n$$

$$^{16}O + n \rightarrow {}^{7}Be + 4p + 6n$$

By electronic capture, ^{7}Be switches to ^{7}Li with $T_{1/2} = 53.3$ days, emitting γ radiation. The production rate of ^{7}Be is about $9 \cdot 10^{-6}$ atoms per gram of oxygen and a second [17].On the territory of Romania it was highlighted the increase of the ^{7}Be concentration due to the nuclear explosion in the atmosphere, produced in China on October 16, 1980 [18]. Regarding the radiological impact, ^{7}Be is fixed by the biosphere and has been identified in the grass.

3.3. Artificial radioactivity

Radionuclides appearing in the atmosphere as a result of human activity give rise to what is called Earth's artificial radioactivity.

The main sources of artificial radionuclides are:

•nuclear explosions;

•continuously controlled emissions of atmospheric effluents (gaseous, as aerosol and liquid);

•accidental emissions at nuclear installations.

3.3.1.Nuclear explosions

Two types of explosive systems based on nuclear energy are known:

• Fission bomb, where the explosion is due to the nuclear fission phenomenon;

• Fusion bomb, where the explosive energy is due to nuclear fusion.

Fission bomb

The nuclear fission consists of breaking a fissionable nucleus (^{235}U, ^{239}Pu) by a neutron and the occurrence of two fission products (intermediate radioactive elements) and at least two neutrons:

$$n + {}^{235}U \rightarrow \nu \cdot n + PF + \gamma$$

where $\nu = 2,5$; PF: fission products; γ: gamma radiation.

The energy released on a fission act is about 200 MeV, in the form of kinetic energy of fission products and the energy of gamma radiation. Neutrons resulting from the fission also produce fission of other nuclei of fissionable material, resulting in other neutrons, what determine an avalanche of nuclear fission reactions, known as chain nuclear reaction. The smallest mass of fissionable element for which chain reaction is self-sustaining is called critical mass. Fission bomb is a nuclear device commonly known as the atomic bomb (or bomb A). The fissile elements usually used are ^{235}U and ^{239}Pu. To initiate the nuclear chain reaction, a neutron source is needed that assembles in the same moment with critical mass. A suitable reflector (i.e., a material with small atomic mass that generally surrounds nuclear fuel) reduces the number of neutrons leaving the reaction zone, which results in a reduction in critical mass. For example, when ^{235}U is fissionable material without reflector, the critical mass is 49 kg, and when there is a 10cm thick Be reflector, the critical mass is 14 kg [16].In the case of ^{239}Pu, the critical mass, without a reflector, is 12.5 kg, and with 32 cm thick Be reflector is 2.5kg [16]. If the multiplication coefficient is greater than 1, i.e. the system is supercritical, the number of neutrons and the released energy increase exponentially, with a generation time of 10^{-8} seconds. It can be proved that for the fission of the nuclei from a kg of ^{235}U, 56 generations are needed and 99% of the nuclear fissions appear in the last 0.05μs [16]. The release of such a high energy, around $5 \cdot 10^{26}$ MeV, in such a short space and a very limited space, is violently explosive and is the basis of the nuclear explosions.

Fusion bomb (with hydrogen or thermonuclear)

The fusion bomb is based on the release of energy in the process of nuclear fusion or nuclear synthesis. This process consists in the union of some light elements, which generates elements with larger mass and releases reaction energy Q (in the

form of kinetic energy of the reaction products). The most interesting from the energy point of view are reactions between hydrogen isotopes, deuterium (^{2}H or D) and tritium (^{3}H or T) [19,20,21]: D+D → ^{3}He + n ,Q= 0,15 (pJ); D+D→ ^{3}H +^{1}H ,Q= 0,64(pJ); T+D → ^{4}He + n, Q=2,82 (pJ); ^{3}He+ D → ^{4}He +^{1}H, Q=1,81 (pJ). Because fusion reactions are produced by increasing the temperature of the reaction medium, they are also called thermonuclear reactions. The uncontrolled fusion reaction was obtained in fusion bombs, also known as thermonuclear bombs or H bombs. Such a device generally consists of two parts: a fusion bomb for obtaining high temperature and a mixture (D,T) which fuses. The fission bomb has a double role: it ensures the high temperature and produces the tritium required for the thermonuclear reaction. It should be noted that apart from tritium, which represents a relatively small radiological risk, the fusion bombs do not use or produce radioactive materials. Even if it has a fission based start system, the high power H bomb is considered "clean" in terms of radioactive pollution, as the contribution of fission and activation products is very low.

The fission and activation products

^{235}U and ^{239}Pu can fission in 40 different ways and give rise to 80 different primary nuclei. Most of the fission products are radioactive and have $T_{1/2}$ ranging from the order of seconds to the millions of years. In most cases, elements resulting from the decay of fission products are radioactive and their daughters are also radioactive, the decay chain leading to a stable element. In addition to fission products, the substances resulting from explosions also contain radioactive elements produced by the interaction of neutrons with the bomb materials and nitrogen from air. For example, neutron interaction with nitrogen results in ^{14}C, with a production rate of $1.5 \cdot 10^{15}$ Bq/kt [16].The plutonium and uranium nuclei that did not suffer the fission process can be found in the environment near explosions and can be transported by the atmosphere and waters at great distances. From the point of view of the environmental radioactivity, the most dangerous are the explosions that occur at the terrestrial surface or at low altitude, although the radioactive fall-out also occur at high altitude explosions. The main fission and activation products released into the medium are: ^{54}Mn, ^{55}Fe, ^{85}Kr, ^{60}Co, ^{89}Sr, ^{90}Sr, ^{95}Zr, ^{131}I, ^{137}Cs, ^{144}Ce. Other radionuclides can be produced from nuclear reactions between neutrons and radioactive constituents of the bomb or found in the atmosphere, rivers and soils (named products of activation).When the explosions occur near the ground, neutrons produce by nuclear reactions a number of radionuclides in the soil: ^{24}Na, ^{32}P, ^{45}Ca, ^{56}Mo, ^{55}Fe, ^{59}Fe. The deposition of radioactive waste from nuclear explosions may occur in the immediate vicinity of the explosion or may be injected into the troposphere or stratosphere. The waste will remain in the troposphere when an explosive device of about 1 kiloton will explode far below the tropopause, but at a height great enough for the globe of fire

not to touch the earth. The depositions of these residues, also called intermediates, will take place at intermediate distances. The bombs exploded at great heights in the stratosphere will cause long-term and planetary depositions. In the case of explosions occurring at the land surface, it is estimated that about 80% of the residues are deposited locally, i.e. near the site of the explosion. The main source of radioactive contamination at planetary level is the long-life isotopes injected into the stratosphere. The constituent particles of tropospheric residues have a size between 1-10μm. Particles with these dimensions and having the activity of $3.7 \cdot 10^{19}$ Bq are called "hot" particles.

3.3.2 Controlled emissions to nuclear reactors: limit values at Cernavoda NPP

In Romania, the National Commission for Nuclear Activities Control - NCNAC is the national authority with responsibilities of regulation, authorization and control of nuclear activities. NCNAC has issued regulations/norms on the radiological safety of nuclear installations, including: individual dosimetry, limitation of radioactive emissions into the environment, monitoring of radioactive emissions, monitoring of radioactivity of the environment in the vicinity of the nuclear power plant. According to the order of NCNAC President no. 14/2000, the general radiological safety requirements for workers professionally exposed, population and environmental conditions imposed the following dose limits for the population [22]: (i) 1 mSv per year for the effective dose; in special situations, NCNAC may authorize a maximum annual limit of up to 5 mSv in one year, provided that the average of the effective doses over a period of 5 consecutive years does not exceed 1 mSv per year; (ii) 15 mSv per year for equivalent dose on the crystalline ; (iii) 50 mSv per year for the equivalent dose on the skin.

On the basis of these annual limits, dose constraints were set for the calculation of the derived exhaust limit (DEL) for gaseous and liquid effluents. Some examples of dose constraints: ^{3}H: 0.0525 mSv in gaseous emissions and 0.0242 mSv in liquid emissions; ^{14}C: 0.0150 mSv in gaseous emissions and $2.27 \cdot 10^{-5}$ mSv in liquid emissions; ^{131}I: $2.88 \cdot 10^{-5}$ mSv in liquid emissions. Regarding effluents released into the atmosphere a few calculated derived limits (GBq/year) are the following [23]: ^{3}H: $3.95 \cdot 10^{6}$; ^{14}C: $5.27 \cdot 10^{3}$; ^{131}I: $8.11 \cdot 10^{-3}$; ^{89}Sr: $1.45 \cdot 10^{-1}$; ^{90}Sr: $1.43 \cdot 10^{-2}$; ^{137}Cs: $1.47 \cdot 10^{-2}$; ^{85}Kr: $4.63 \cdot 10^{4}$; ^{133}Xe: $4.06 \cdot 10^{5}$. For liquid effluents, examples of calculated DEL (GBq/year) are the following [23]: ^{3}H: $1.97 \cdot 10^{6}$; ^{14}C: $8.94 \cdot 10^{-1}$; ^{131}I: $9.07 \cdot 10^{-1}$; ^{137}Cs: $4.78 \cdot 10^{-2}$.

The real exhaust limits are much lower than those calculated with dose constraint. For example, in the case of tritium, in 2010 the real evacuation limit was 6.31% of DEL, in 2011 it was 3.54%, and in the case of ^{14}C, in 2010 it was 4.12% and in 2011 it was 2.04% of DEL [24].

3.3.3 Accidental emissions to nuclear reactors

Generally, the accidents at a nuclear power plant can be divided as follows: a) reactivity accidents; b) accidents caused by the damage to the primary circuit; c) accidents caused by the handling of nuclear fuel; d) site-related accidents (earthquakes, floods, etc.). The first two types of accidents stem from the inability of the heat transport system to cope with the high rate of release of energy from nuclear fuel. In the reactivity accidents, the reactor becomes overcritical non-controllable, so that the cooling system, although operating normally, can not cope with the massive release of heat from the combustible bars. The possible accidents are explosions due to vaporized fuel and high pressure water vapors resulting from vaporization of the heat agent. The most serious accident is the loss of electric power to the cooling pumps at all the loops forming the primary circuit. The fourth category of accidents (d) includes those that occur as a result of external factors or environmental-induced phenomena: fall of an airplane, intentional attack, wind, floods, landslides, earthquakes. Earthquakes are the most carefully analyzed since the ground movements have direct effect not only on the tire, but also on each system in the plant. The history of nuclear power is marked by the existence of nuclear accidents of special intensity, accompanied by material destruction, environmental contamination and irradiation of technical personnel and population. At the same time, the accidents were moments to re-evaluate the methods of designing the reactor cores, of ensuring the operational safety and control of the nuclear power plants. The most known are accident from Windscale (England, 1957), Three Mile Island (S.U.A., 1979), Chernobyl (Ukraine, 1986), Fukushima (Japan, 2011).

The Windscale accident (England, 1957)

At Windscale, two nuclear reactors with natural uranium, graphite moderator, and air cooling agent were used to produce plutonium. Due to the excessive accumulation of heat in the graphite, melting of the fuel has occurred. The accident lasted for 4 days and was detected by a radioactivity monitoring station located 1 km from the reactor stack. Examples of radionuclide emission activities in the atmosphere [25]: ^{131}I: $7.4 \cdot 10^{14}$ Bq; ^{137}Cs: $22 \cdot 10^{12}$ Bq; ^{133}Xe: $12 \cdot 10^{15}$ Bq .

Accident at Three Mile Island (S.U.A., 1979)

At Three Mile Island there are 2 nuclear power plants , each with a power of 850 MWe. The reactor works with enriched uranium and light water under pressure. The reactor core contains 100 tons of uranium under the form of bars with a height of 3.6 m. The accident was a loss of cooling agent. In the first 10 hours of the accident, a large amount of ^{2}H was produced in the reactor core zone as a result of the reaction between the steam and the sheaths of zirconium of the nuclear fuel. It is estimated that 90% of the fuel bundles have suffered sheath defects. Emissions of iodine in the atmosphere were in the range:$4.8 \div 6.3 \cdot 10^{11}$Bq and noble gases in the range: $8.9 \div 48.1 \cdot 10^{16}$ Bq [26].

The Chernobyl accident

In April 1986 occurred at Chernobyl (Ukraine) the worst accident in the history of nuclear energy (melting of reactor core and thermal explosion).The radionuclide emissions were particularly high and affected many countries, including our country. Some examples of total emissions of the most important radionuclides [27]: ^{85}Kr :3,3·10^{16}Bq; ^{133}Xe:1,7·10^{18} Bq; ^{131}I: 2,6·10^{17} Bq; ^{137}Cs: 3,77·10^{16} Bq; ^{90}Sr: 8·10^{15}Bq; ^{239}Np:4,2·10^{15}Bq; ^{238}Pu:3·10^{12}Bq; ^{239}Pu:2,5·10^{13} Bq; ^{240}Pu: 3,6·10^{13}Bq; ^{241}Pu: 5,1·10^{15}Bq.In the case of atmospheric aerosols, the maximum levels for ^{131}I with values of 103 Bq / m3 and 63Bq/m3 were reached on May 1, 1986, at Ceahlau Toaca Station, respectively with values of 17 Bq/m3 and 14 Bq/m^3 (for ^{131}I) at Fundata Braşov County [28]. With regard to the integrated concentration of ^{137}Cs in aerosols, from about 10^6 Bq.s/m^3 in May 1986 it dropped to less than 10^5 in 1987, recovering from 1991 to the value before the accident (about 200 Bq.s / m3). The average values of the ^{137}Cs concentration in the uncultivated soil samples were about 350 Bq/kg, with maximum values exceeding 1000 Bq/kg in the north of Gorj county. High values of ^{137}Cs in uncultivated soil were recorded in Toaca-Ceahlau, Târgu Mureş, Gheorghieni, Axente-Sever, Parâng with extremes ranging between 7 and 2050 Bq/kg dry soil.

The accident from Fukushima

The severe nuclear accident at Fukushima Daiichi was due to an earthquake followed by a tsunami (huge waves over 15m high) on March 11, 2011, and determined destruction of equipment, melting of nuclear materials and evacuation of gaseous and liquid effluents. The institution responsible for the management and operation of the plant, Tokio Electric Power Company, claims that the total ^{131}I, ^{134}Cs and ^{137}Cs activities were 511 PBq, 13.5 PBq, and 13.6 PBq, respectively[29].

4. Results and discussions

In this section will be disccused the results regarding the fractal characteristics of different components of the environmental radioactivity that are presented in different papers.

4.1. Fractal characteristics of the outdoor, indoor and in soil radon

•Paper[5]

►*Outdoor ^{222}Rn and ^{220}Rn time series*

The fractal properties of the ^{222}Rn/^{220}Rn time series were studied using Hurst's rescaled range analysis, as well as the box counting method.

Assuming radioactive equilibrium between $^{222}Rn/^{220}Rn$ and daughters, the measuring method was based on aerosol collection on filters by means of an air filtering device with the aspiration head 2m above the ground.The filter activity was determined using low background beta global measuring equipement from Nuclear Enterprises with G-M counter tubes, with 2 counts min^{-1} background in anti-coincidence. As a reference standard, $^{90}Sr/^{90}Y$ was used. The study was carried out on a set of 4200 activity concentration values of atmospheric radon and thoron, obtained by 4 daily measurements over a period of 3 years (1990-1992) at the Observatory of Atmospheric Physics located near Bucharest. During this period, 5-hour aerosol samples were taken daily between 02-07, 08-13, 14-19, 20-01 GMT. The 5 h aspiration time was chosen because it was intended to determine the presence of artificial activity as well. Statistical errors were between 0.5 and 2%. Errors due to the reference standard, to the air flow rate determination and the filter efficiency were estimated at a maximum value of 20%.

►*Results and discussions*

The Hurst exponent (H)and the fractal dimension of the time series have been estimated with computational programs developed for these cases. Since H is a statistical parameter, it can be determined correctly from the analysis of a data set containing about 2500 values. This condition is met because we have shown that the radon and toron sets contain 4200 values.

Two sets of data, with 4000 values each, were generated for testing the computational programs: one containing deterministic data (H = 1, $D_H = D_B$ = 1) and the other, Gaussian random data (H = 0.5, $D_H = D_B$ = 1.5).The deterministic data set was obtained by solving the time-dependent diffusion equation at the height z = 1 m and a diffusion coefficient equal to $1m^2s^{-1}$ .The random data set was obtained using the Muller method that generates data with normal (Gaussian) distribution with zero mean and unit variance. As expected, for deterministically generated data set the least square fit gave H=0.998±0.0002. For the data set with Gaussian statistics, the obtained Hurst exponent was H=0.479 ±0.029, D_H =1.521±0.003, and D_B =1.509±0.023.There is a good agreement (D_B=□D_H) between the two ways of estimating the fractal dimensions of a time series. The errors are the standard deviations estimated from the covariance matrix obtained in the fit.

The above values prove that the geometrical properties of a time series of an observable may provide reliable information on the nature of the physical system that has produced the respective measured data set. In Fig. 3 one presents the Hurst exponent for the ^{222}Rn time series. The least square fit resulted in H =0.809 ±0.005 and the corresponding fractal dimensions were: D_H =1.191 ±0.005 and D_B =1.104±0.029 (Fig. 4).

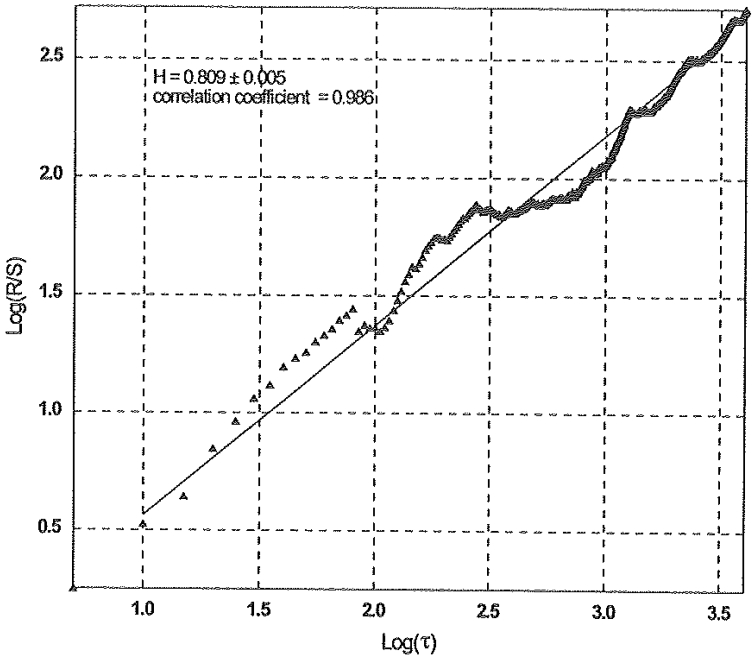

Fig. 3. ^{222}Rn –Hurst exponent.

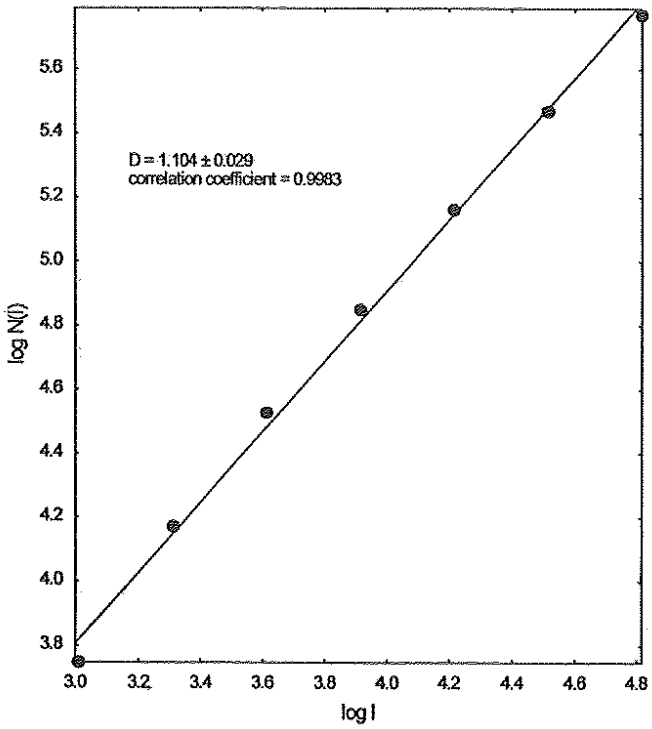

Fig.4. ^{222}Rn - Box counting dimension.

The fractal dimension from Fig. 4 is obtained by the method of calculating the numbers of values from the squares that approximate the distribution, making use of relation (14). The Hurst exponent for the ^{220}Rn time series is given in Fig. 5 and has the value H=0.896±0.006.

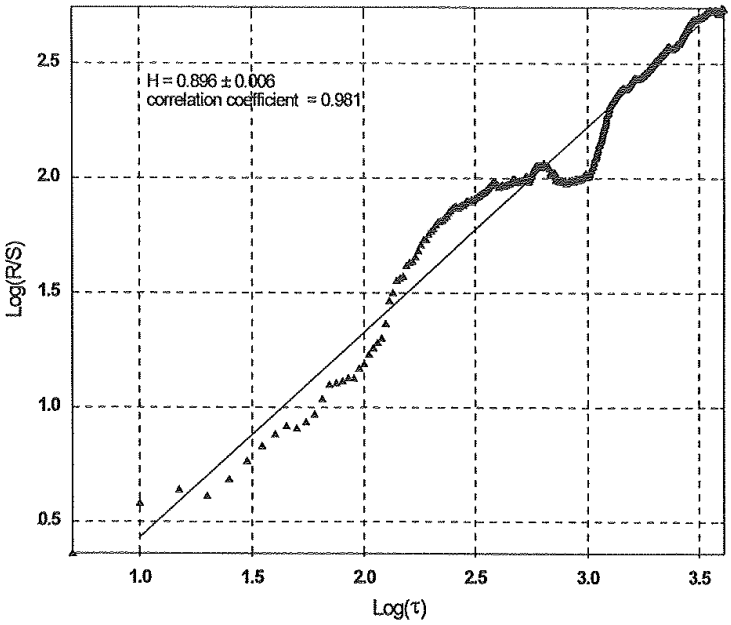

Fig. 5. ^{220}Rn - Hurst exponent.

The two fractal dimensions were D_H =1.104±0.006 and D_B =1.103±0.03. The Hurst exponent for ^{222}Rn and ^{220}Rn time series lie in the same range of values as many natural phenomena (atmospheric temperature, rainfall, water flow).The high values of H indicate that ^{222}Rn and ^{220}Rn statistics are strongly non-gaussian.The concentration ranges of the two radionuclides are directly dependent on the turbulent diffusion process which is characterized by a Hurst exponent greater than 1/2. Since the values of H are significantly greater than 1/2, one may conclude that the ^{222}Rn and ^{220}Rn concentration fields exhibit persistence and, consequently, a "memory" effect of the previous states. The non-integer fractal dimensions of the ^{222}Rn / ^{220}Rn time series demonstrates that mechanism underlying the concentration dynamics of these radionuclides in the atmosphere is intrinsecally non-linear. The main consequence of this mechanism is the non-predictability of the variation of concentration in the classical sense. The attractor of such a physical system is chaotic. Although deterministic, the dynamics of these systems reveal chaotic or irregular behavior, caused by a sensitive dependence on the initial conditions-a feature of the atmospheric states. Since the fractal dimensions have noninterger values, the ^{222}Rn / ^{220}Rn time series are fractals.

•Paper[30]

►*Outdoor and indoor ^{222}Rn time series*

In this paper are examined the fractal properties of the time series of outdoor and indoor ^{222}Rn using Hurst's rescaled range analysis as well as other physical quantities specific to the deterministic chaos. The Hurst exponent lies in the region of 0 to 1; if the H is close to 0.5, the time series point out random and uncorrelated data, or successive steps are independent. Radon concentration measurements were made at three different locations (site A: Tiborjanci, indoors, living room; site B: Valpovo, outdoors; site C: Valpovo, indoors, basement) with an Alpha Guard PQ 2000, as well as the barometric pressure and temperature of the air. The measurements were carried out in 10 minutes intervals in May (site A; 4332 intervals), June (B; 4038) and September 2002 (C; 2269), and the mean radon concentrations of 31.1 Bq/m^3, 13.6 Bq/m^3 and 121.2 Bq/m^3, were obtained.

►*Results and discussions*

The Hurst exponents for the radon in the three sites have the following values: site A, H=0.16; site B, H=0.15; site C, H=0.23. In case of barometric pressure the values of H are: site A, H=0.74; site B, H=0.71; site C, H=0.79 and in case of temperature these values are: site A, H=0.61; site B, H=0.86; site C, H=0.53 .

The Hurst exponent for radon was small and less than 0.5, that indicated anti-persistent behavior, this means that an increasing trend in the past implied a probable decreasing trend in the future, and conversely; this behavior was particularly specific to the outdoor radon, that had the least value of H (= 0.15).The Hurst exponent (H = 0.5) indicates random and uncorrelated data of the temperature time series in the basement. The high values of the Hurst exponent ($0.5<H<1$) for pressure and temperature indicated persistent behavior, or an increasing trend in the past implied on the average a continued increase in the future, and conversely for decreasing trend.

•Paper[31]

►*Time series of outdoor, indoor and in soil ^{222}Rn*

This paper presents the fractal characteristics of the time series of ^{222}Rn concentrations estimated by making use of Hurst exponent and of other physical quantities describing the deterministic chaos. Radon concentrations were measured with an Alpha Guard PQ 2000 detector (Genitron Instrument, Germany), outdoors (O), indoors (I) and in soil (S) at a location in Valpovo (a town near Osijek). The sites O and S were positioned outside in the garden, 1 m above the ground and 0.8 m deep in the soil, respectively, while the site I was in a closed basement room of a single house. In the same time, the atmospheric

temperature and pressure were measured. At each site, the Alpha Guard detector was set to authomatically read and make a record of the number of counts every 10 minutes. Many readings of the radon concentration were carried out: in June (site O; 2835 readings), in July (site I; 3679) and in September (site S; 2967), in the year 2004.

They were obtained the following mean radon concentrations: 16.4 Bq/m3, 66.7 Bq/m3 and 25.01 kBq/m3.

►*Results and discussions*

The time variations of the radon concentration in the soil (site S) and the barometric pressure, are presented in Fig. 6.

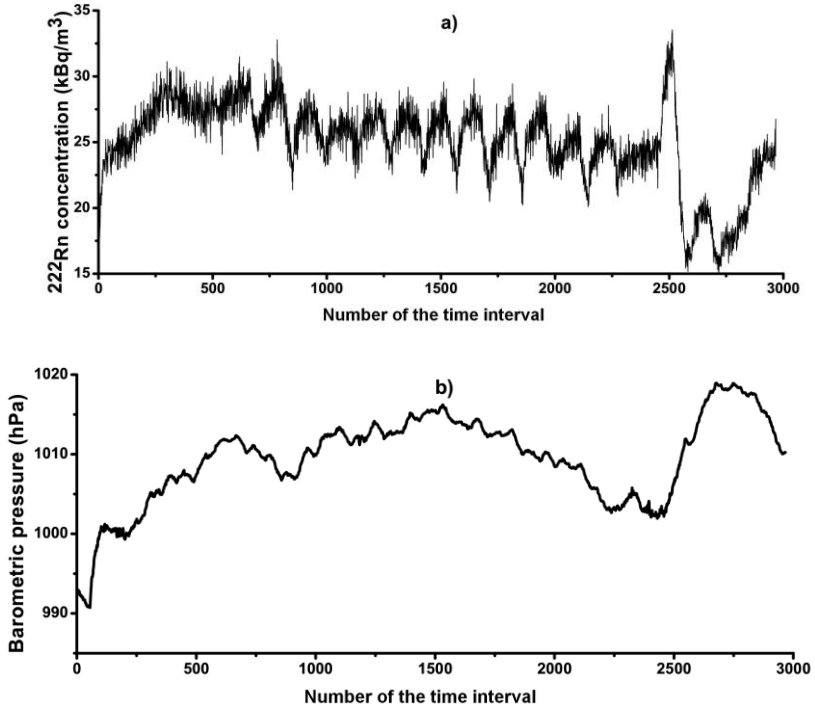

Fig. 6. Variation of the radon concentration in the soil versus the number of 10 min intervals (a), as well as variations of the barometric pressure (b).

A particular radon signal appeared around the 2500th time interval at the site S that previously was interpreted as a radon anomaly when searching for earthquake precursors. The radon signal, after the peak of 33.53 kBq/m^3, had a minimum that typically corresponded to the shape of a radon anomaly preceding an earthquake coming in about three weeks. Studies of the radon concentration in soil have

shown a barometric effect. Thus, it has been found a negative correlation between the radon concentration in the soil and the barometric pressure.

This may be seen as changes of the radon concentration and atmospheric pressure presented in Figs. 6a and 6b about the 2500th time interval.

The decrease in barometric pressure corresponds to an increase in the radon concentration, and conversely. The calculation of the Hurst exponents for the three series of measurements of radon concentration (at the sites O, I and S) has provided the following results: the site O, H=0.13; site I, H=0.12; site S, H=0,2.

In case of barometric pressure the corresponding values are the following: the site O, H= 0.67; site I, H=0.70; site S, H= 0,71, and in case of temperature the respective values are: the site O, H=0.88; site I, H= 0.50; site S, H=0,72.

The Hurst exponent for radon was small and less than 0.5, pointing out anti-persistent behaviour, i.e. an increasing trend in the past implied a probable decreasing trend in the future, and conversely (Fig. 7).

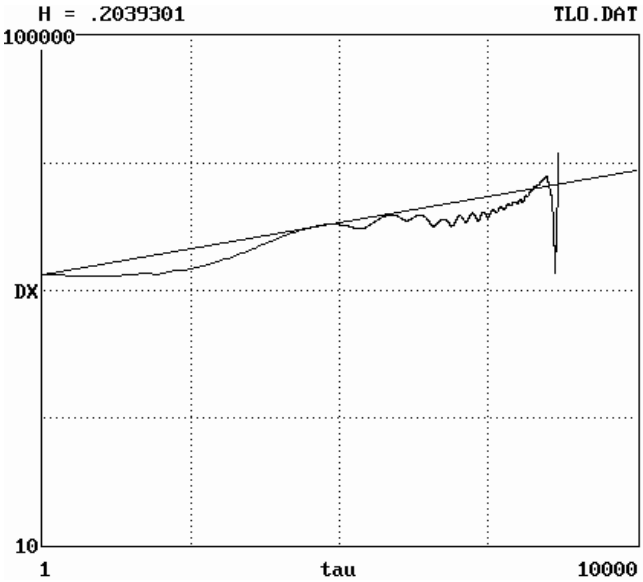

Fig. 7. The calculated values of the Hurst exponent for the time series of radon in the soil.

The Hurst exponent (H =0.5) of the temperature time series indicates a random dynamics of these data in the basement (site I).

The high values of the Hurst exponent($0.5 < H < 1$) for pressure and temperature point out a persistent behaviour, i.e., an increasing trend in the past implied on the average a continued increase in the future, and conversely for a decreasing trend.

•Paper[32]

►*Indoor ^{222}Rn time series*

The analysis of the behavior of radon time variations in indoor air, indicates that this gas is a radioactive tracer of a complex and dynamical system where the influencing variables continuously interact, some of them in a chaotic but also deterministic way, as is the case of temperature and atmospheric pressure.

In this paper one applies the fractal analysis to a time series of radon variations registered in a house at Angera (Italy) in 1986-1987, with the purpose to calculate the fractal dimension of the attractor of a complex system radon-indoor environment. The measurements, registered every 30 minutes, are expressed in counts (relative values) because, in this form, they are directly proportional to radon concentration.

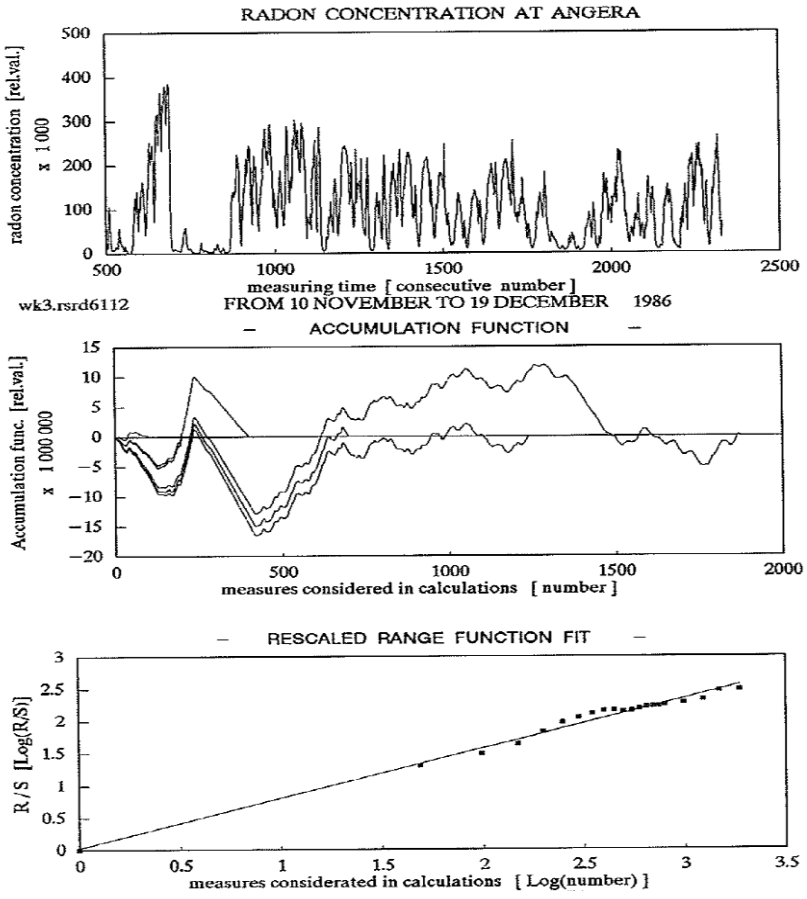

Fig. 8. Hurst exponent obtained by the rescaled range analysis.

Two methods are presented for calculating the fractal dimension: rescaled range analysis used to estimate the Hurst exponent and box counting method.

Using the relationship between Hurst exponent and fractal dimension in case of self-affine records one may deduce the corresponding fractal dimension.

►*Results and discussions*

The set of radon data measured in the period 10 November to 19 December 1986, in the mentioned house and the results regarding accumulation function and rescaled range function fit with the obtained Hurst exponent are presented in Fig. 8.

The average value of the Hurst exponent is $< H >=0.77\pm0.04$, that is significantly greater than 0.5. This denotes that phenomenon statistics is really non-gaussian. The corresponding fractal dimension has the value $D_H=1.228$.

The box counting method has been apllied to the radon time series of many periods using square grid sides of 2.5+3.0+5.0+8.0mm.

Making use of the radon data (number of data 1450) from the month of April 1986, the box counting method has provided the the value 1.418 for the fractal dimension (Fig.9).

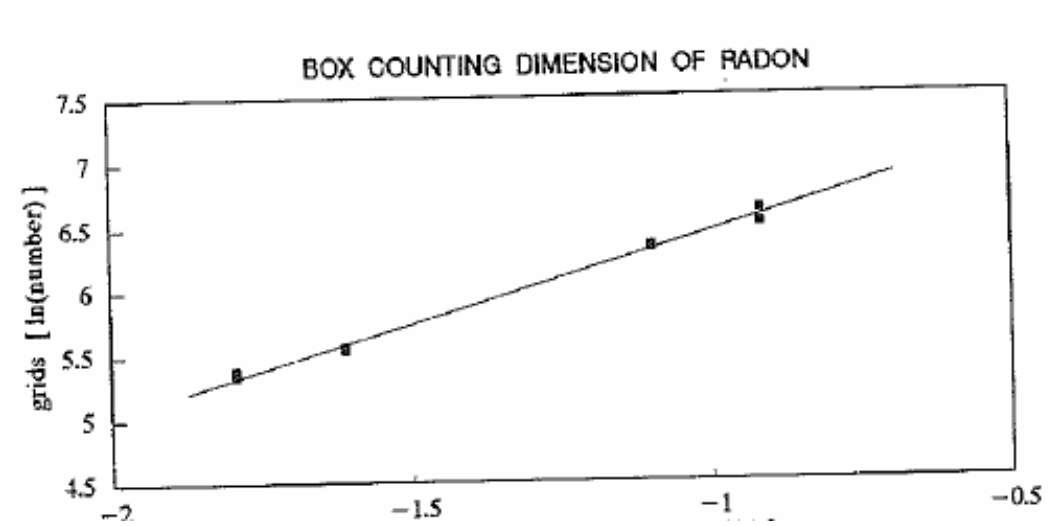

Fig. 9. Fractal dimension calculated with data from April 1986($D_B=1.418$).

The average value of the fractal dimension for radon data from the three periods (April 1986, May 1986, January1986) $< D_B >=1.24\pm0.16$, is congruent with that of Hurst method $< D > = 2 - < H > =1.23\pm0.04$, derived from equation for self-affine sets.

•Paper[33]

► *Soil ^{222}Rn gas time series*

Measurements of ^{222}Rn gas concentration have indicated rising concentrations on many fracture and fault zones in soil, air and ground water.

Also, the measurements have shown that concentration of ^{222}Rn changes depending on the earthquake magnitude and the geological structure of the region.

High radon concentration is common in soil under deep cracks such as geological faults and active volcanoes.

An earthquake may increase the mobility of radon gas in the soil.

Existing studies have shown that a few weeks or months before occurrence, the earthquake might be sensed due to radon concentration exchange in soil gas.

Changes in radon concentration levels are visible as earthquake precursors.

The variations in the radon gas level along the fault lines have non-linear behaviours and they are used for the earthquake prediction studies.

In this paper, 70272 soil ^{222}Rn gas measurements are considered and the chaotic methodologies are used to predict the non-linear behaviours.

The application is performed for data from Kozan and Yakapinar regions near the East Anatolian Fault Zone, Turkey.

The non-linear prediction through chaos study methods is applied to recorded data from 1 January to 31 December 2009 and the continuous soil radon measurements are taken at 15-min intervals for one year in the study regions.

In this study, ^{222}Rn gas is measured with an alpha detector, Alphameter 611 (Alpha Nuclear Inc. Canada) based on a 400 mm^2 silicon junction diode, immersed in a sensing volume open to the geo-gas.

►*Results and discussions*

Using the rescaled range analysis, the obtained values of Hurst exponents were 0.55 for data from the Kozan region and 0.60 for the radon data from the Yakapinar region.

Because the Hurst exponent is in the range $0.5 < H < 1$, the system has fractal chaotic structure, and hence, the system is dependent on the initial conditions.

•Paper[34]

►*Time series of ^{222}Rn exhalation rate*

The mining and processing of uranium ores produce large amounts of mill tailings, which are normally disposed as tailings impoundment on the surface of special areas, which are generally valleys near the uranium mines.

Generally, these tailings are large volumes of low-level radioactive materials and might be the sources of the radioactive gas ^{222}Rn.

As radon was produced by α-decay of radium in solid media-like soil, rocks and mines, the natural properties of these media may play an important role in radon behaviors.

In order to investigate whether the internal mechanisms can cause the radon nonlinear variation, in this study, was measured radon exhalation rate of uranium tailings in a laboratory under steady microclimatic conditions.

The obtained time series of radon exhalation rates have been analyzed using fractal and chaotic methods to study the dynamics of radon exhalation from uranium tailings.

The uranium tailings samples were collected from the 272 Plant, in Hengyang city, Hunan Province, China.

The particle size distribution and chemical composition of the tailings were determined from 10Kg tailings that were homogeneously mixed.

The grain sizes of tailings mainly range from 0.005 mm to 5 mm.

The tailings were loaded into two cylindrical PVC columns having 1.5 m in height, and 0.3 m in inner diameter. These two columns contain 235.65 kg and the 249.3 kg tailings and have been labeled as SZ-1 and SZ-2, respectively.

Radon exhalation rates on the surface of tailings in SZ-1 and SZ-2 were continuously measured for 20 days in an air-tight laboratory; the corresponding readings were made every 90 min.

At the same time, in the laboratory it were recorded the temperature, atmospheric pressure and relative humidity.

Radon exhalation rate was measured by accumulator technique, using FD-125 Rn measurement instrument (Beijing Nuclear Instrument Factory, China).

►*Results and discussions*

Figure 10 shows the time dependent variations of radon exhalation rate of the two columns, proving that both time series present sharply fluctuation.

The radon exhalation rate of SZ-1 is 0.154 -5.245 $Bqm^{-2}s^{-1}$, while that of SZ-2 is 0.103 - 5.955 $Bqm^{-2}s^{-1}$.

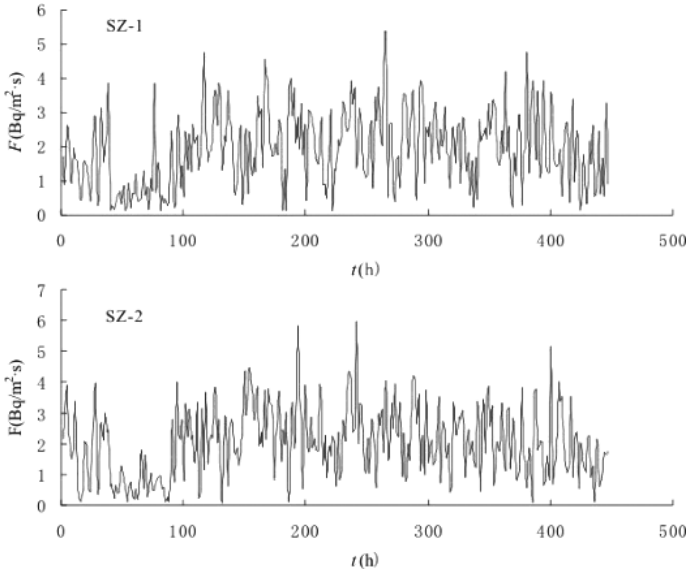

Fig.10. Measured values of radon exhalation rate.

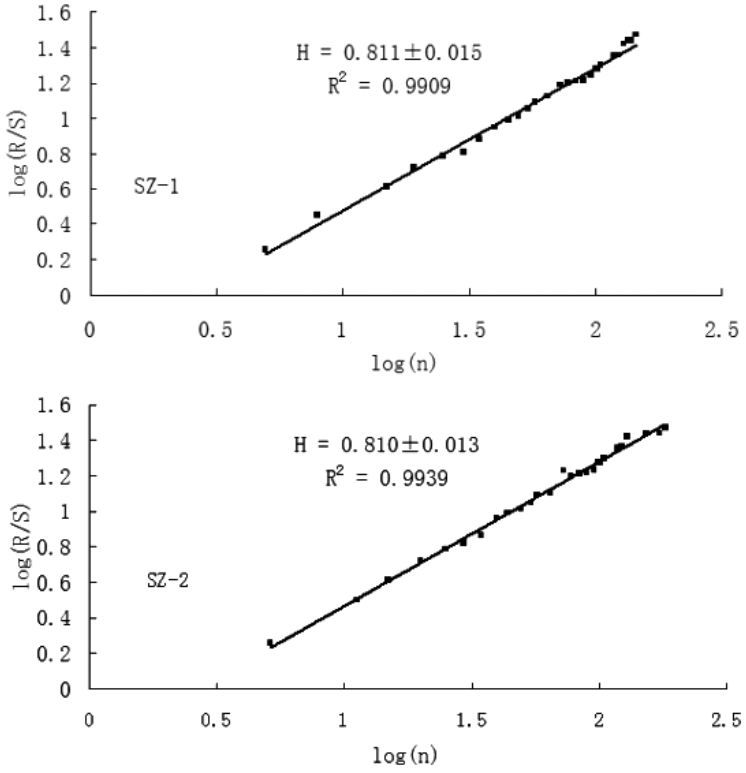

Fig 11. The Hurst exponents for radon exhalation rate.

Making use of the rescaled range analysis method were calculated the Hurst exponents for the time series of radon exhalation rate from each column. The results are presented in Fig.11; *n* is the number of the sampling interval.

The least-square fitting of log(*R/S*) and log(*n*) for the two time series of radon exhalation rate are shown in Fig. 11, indicating that the values of *H* of SZ-1 and SZ-2 are 0.811±0.015 (*D* = 1.189±0.015), and 0.810±0.013 (*D* = 1.190±0.013), respectively. The values of *H* being much larger than 0.5, prove that the non-random variation of radon exhalation from uranium tailings probably exhibits persistence, while the non-integer fractal dimensions indicate that radon exhalation is intrinsically nonlinear. One can conclude that the internal factors, which include heterogeneous distribution of radium, and randomness of radium decay, as well as the fractal characteristics of the tailings, can determine the chaotic dynamic of radon exhalation from the tailings.

•Paper[35]

►*Indoor ^{222}Rn time series*

The application of fractal methods allows studying the chaotic nature of indoor radon concentrations.

The main characteristics of the fractal techniques employed in this paper are briefly described. These fractal methods have been applied to three indoor ^{222}Rn time series (consisting of N measurements) from three different locations in Austria. Two of the rooms, a kitchen in Strasswalchen (N = 2275 in 10 minutes intervals) in spring of 1997, with an average radon concentration of 30 Bqm^{-3}, and a working room in Traun (N = 3442 in 1 hour intervals) in spring of 1998, with an average radon concentration of 415 Bqm^{-3}, were in brick built private houses. The third room, a radiation laboratory at the Institute of Physics and Biophysics in Salzburg (N = 6867 in 10 minutes intervals) in spring of 1998, with an average radon concentration of 16 Bq m^{-3}, is housed in a concrete building. All radon measurements were made with an AlphaGuard PQ 2000. Temperature and barometric pressure were measured simultaneously in each room and these measurements (and related quantities) were analyzed by the same fractal methods as those applied to the radon concentrations. In the present study it is assumed that the measure of the degree of correlation between these meteorological parameters and their corresponding radon concentrations is the similarity of their fractal dimensions.

►*Results and discussions*

The values of the different fractal characteristics demonstrate that indoor radon concentrations in all three rooms exhibit the features of chaotic systems. The

Hurst exponents for those three places of measurement have the following values: kitchen (Strasswalchen): 0.19(±0.04), working room (Traun): 0.38(± 0.08), laboratory (Salzburg): 0.02(±0.01). While the radon data in two rooms (kitchen, radiation laboratory) were recorded every 10 minutes, the radon concentrations in the working room were measured in 60 minutes intervals. To verify the effect of the length of the time steps on the results of the fractal analyses, the 10 minutes data were converted into average 1 hour values and then analyzed again. The obtained fractal characteristics for the modified data set were not different from those derived from the original data set.

4.2. Fractal characteristics of the radionuclides occuring during the nuclear accidents

•Paper[36]

► *Radioisotope pollution patterns by nuclear power plant accident*

The radioisotope pollution exhibits two types of patterns: dry and wet depositions due to nuclear power plant accidents. Two surface pollution patterns were analysed by the fractal method.

Because during Fukushima nuclear power plant accident was no rain, the surface pollution by wet depositions did not occur, but white crystals were observed on the surface. Fractal analysis was carried out for the spatial distribution patterns of radioisotopes on the surface to judge the types of depositions. As a reference, Chernobyl nuclear power plant accident was checked for the spatial distribution patterns of radioisotopes on the surface. The objective patterns by fractal analysis were the surface pollution maps in Fukushima and Chernobyl, Abukuma river watershed map, and NOAA/AVHRR.

►*Results and discussions*

Fractal is characterized by fractal dimensions, which distribute 1 to 2 in two dimensional images.

In fractal analysis, the objects were a soil pollution map in Fukushima accident(2011), a soil pollution map in Chernobyl accident (1991), Abukuma river watershed map, and NOAA/AVHRR data.

In fractal dimension calculation, the box counting method was selected for binarized images. By applying a relationship similar to (14) one calculates the fractal dimensions for the soil and water pollution maps and for NOAA-AVHRR data.

The calculated values of the fractal dimensions are the followings: 1.83, for soil pollution map in Fukushima, 1.53 for soil pollution map in Chernobyl ,1.83 for Abukuma river watershed and 1.56 for NOAA/AVHRR with cloud image.

•Paper[37]

► *^{137}Cs fallout pattern resulting from Chernobyl accident*

It has been proved that multifractal analysis can be a useful tool for determining the ability of a monitoring network to actually detect certain fallout phenomena. Multifractals are related to the statistical distribution of measures on a geometrical support: a line, a surface, a volume, or a fractal, for instance. Multifractals are formed by an interwoven of fractal subsets with different scaling exponents. In a mentioned paper one shows that sub-nets formed by the points of the basic net with contamination levels above a given threshold C [kBq m^{-2}] can also be described as fractal systems, with dimensions D(C), forming a multifractal structure up to a level of C=20 kBq m^{-2} .

►*Results and discussions*

In this paper one investigates the fractal structure of the network of 1881 monitoring points which were used to determine the fallout pattern of ^{137}Cs in Austria. The calculated fractal dimensions(Dn) of the^{137}Cs fallout pattern decreases with increasing threshold(C_0), as follows: $C_0 \geq 0$ kBqm^{-2}, Dn=1.426±0.022; $C_0 \geq 25$ kBqm^{-2}, Dn=1.231±0.026; $C_0 \geq 50$ kBqm^{-2}, Dn=0.972 ±0.015; $C_0 \geq 75$kBqm^{-2},Dn=0.788±6.027; $C_0 \geq 100$kBqm^{-2} ,Dn=0.706±0.047.

The corresponding fractal spectrum, namely, the function Dn(C_0) is monotonously decreasing up to a threshold value C_0 of about 90 kBqm^{-2}. Deviations from this behaviour at higher C_0 levels result from the paucity of points with ^{137}Cs contamination levels above this value.

•Paper[38]

► *^{137}Cs cumulative soil deposition after the Chernobyl accident.*

This paper deals with the modeling of ^{137}Cs cumulative soil deposition measured in some European Countries after the Chernobyl accident. The data come from the *Radioactivity Environmental Monitoring* (REM) data base, organised by the *Joint Research Centre* (JRC) of Ispra (Italy).

The purpose of paper is to investigate whether or not the Chernobyl fallout has fractal properties, and to use these properties in order to estimate the radioactive concentration in sites where no experimental data are available. Closely related to fractals are the hyperbolic probability distribution, which is a useful theoretical framework for modeling phenomena showing anomalous fluctuations like, e.g., the hot spots of radioactive concentration. The fractal properties vary by changing the contamination level, and one may define a spectrum of fractal dimensions that is called a multifractal spectrum.

To justify the application of multifractals it is necessary to verify the existence of a possible (asymptotic) hyperbolic probability distribution of the radioactive concentration R, viewed as random variable, i.e.: $P(R > r) = r^{-\delta}$ for large enough R, where P means probability and δ is the hyperbolic characteristic exponent.

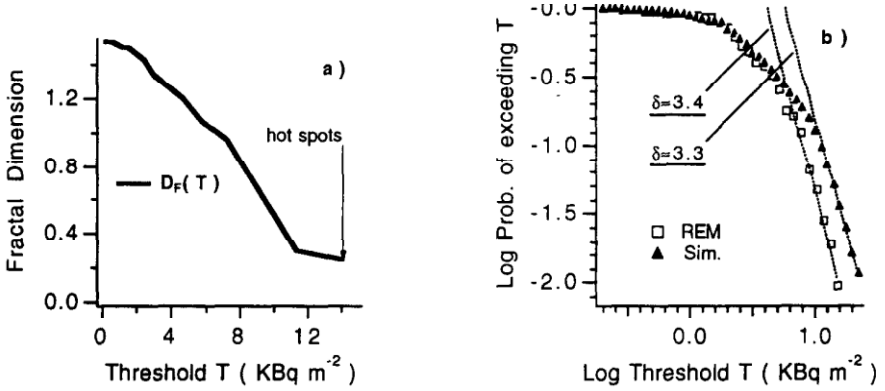

Fig. 12. Multifractal features of ^{137}Cs cumulative soil deposition data in Czechoslovakia. (a) The multifractal spectrum $D_F(T)$. (b) The asymptotic hyperbolic distribution of the REM data (empty squares) and of the corresponding multifractal simulation (full triangles); the dashed lines represent the asymptotic fits, and the hyperbolic exponent δ is estimated by the value of the slope.

► *Results and discussions*

As it was mentioned, the multifractal analysis provides the multifractal spectrum $D_F(T)$ and the hyperbolic exponent δ of the ^{137}Cs cumulative soil deposition data. In Fig. 12 one presents the multifractal spectrum $D_F(T)$ calculated for the data set of Czechoslovakia. As expected, the fractal dimension decreases with increasing threshold T, i.e. the data show different fractal behaviour for different levels of radioactivity. In particular, the hot spots lie in the region corresponding to highest radioactive concentrations and lowest fractal dimensions, i.e. they are very sparse in space.

5. Conclusions

The present paper has three main components: theory of fractal model used in different scientific domains, detailed presentation of the environmental radioactivity and the analysis of papers applying the theory of the fractals for describing the nature of the dynamics of environmental radioactivity. The following conclusions are presented in the reviewed papers:

-[5] The fractal dimension of a time series is accurately determined by using R/S analysis, as well as the box-counting procedure. It proves the turbulent nature of the atmospheric diffusion process as well as the irregular time dependence of soil exhalation variations. The more pronounced persistence of ^{220}Rn than that of ^{222}Rn can be explained by the fact that the ^{220}Rn concentration field is less sensitive to the turbulence intensity variations.

Because the fractal dimensions have non-integer values, the $^{220}Rn/^{222}Rn$ time series are fractals. Therefore, these two gases are tracers of a dynamic system whose variables continuously interact, some of them in a chaotic, but also deterministic way.

-[30] The Hurst exponent (*H*) is calculated for three radon time series (one in the living room, one outdoors and one in the basement), as well as for the time series of barometric pressure and temperature. In case of the in basement data for temperature, the corresponding time series has H =0.5, what means that the temperature data are random and uncorrelated. The Hurst exponent for radon was small and less than 0.5, what indicated anti-persistent behavior. This behavior was mainly specific to the outdoor radon, that had the least value of *H*(=0.15).The high values of the Hurst exponent ($0.5<H<1$) for pressure and temperature indicated persistent behavior.

-[31]The use of the fractal methods to three radon series of measurements (outdoors, indoors and in the soil), and to the barometric pressure and temperature provided the values of the Hurst exponents (*H*). The Hurst exponent, *H*=0.5, indicates random dynamics of data of the temperature time series in the basement (site I), what indicates the absence of deterministic chaos. For radon, *H* is small and less than 0.5, indicating anti-persistent behaviour; this behaviour was most expressed for the indoor radon, that had the smallest value of *H*(= 0.12). For pressure and temperature, the high values of the Hurst exponent ($0.5 < H < 1$) indicated a persistent behavior.

-[32] The exponent *H*, pertinent with studied time series of radon concentrations, is congruent with the values encountered in other natural phenomena. It may conclude that this system can be considered deterministic and chaotic. Thus, it is possible for the studied time series to be represented with a suitable phase-space attractor, whose fractal dimension is equals to 1.2. According to the paper conclusions the indoor environment is intrinsically noisy, with measurements being susceptible to noise contamination from a variety of external sources, such as use of doors, external winds, and others. The presence of noise restricts the observability of possible scaling.

-[33]The chaotic behavior of soil radon gas has been studied through a set of nonlinear analyses techniques for the data recorded. The analyses of nonlinear time series are performed to understand the propagation of ^{222}Rn concentration in the soil and confirm the chaotic structure of the data sets. The conclusion of chaotic time series analyses points out the chaotic behavior of the complex dynamic systems concerning radon emanation and transport in natural sub-surface systems. The results obtained make evident a robust chaos signature of the radon time series.

-[34] The dynamical nature of radon exhalation from uranium mill tailings and the underlying mechanism have been studied using theoretical and experimental methods. The values of the Hurst exponents for radon time series are larger than 0.5, indicating that non-random variation of radon exhalation rate from uranium tailings is persistent.

The internal factors, including heterogeneous distribution of radium, and randomness of radium decay, as well as the fractal properties of the tailings, can lead to chaotic dynamics of the radon exhalation from the uranium tailings.

-[35]Analysis of chaotic time series has greatly improved the understanding of chaos in experimental physical systems by allowing multi-dimensional dynamical information to be recovered from a time series of measurements of a single variable.

In this way the strange attractor of a chaotic system can often be extracted from a time series of measurements of a single variable, in our case the radon concentration.

The fractal analysis of ^{222}Rn time series allows distinguishing between chaotic behavior (deterministic chaos) and noise (random fluctuations).

This information is used to understand the physical mechanisms behind the chaotic behavior, such as the dependence of indoor radon concentrations on meteorological factors or ventilation conditions. Indoor ^{222}Rn concentrations do indeed exhibit features which are specific to the chaotic systems.

The studies of radon time series from this paper, suggest low dimensional chaos for the kitchen, high dimensional chaos for the working room and chaos with additive noise for the radiation laboratory.

The similarity of fractal dimensions between radon concentrations and meteorological parameters may be considered as a measure of their degree of correlation.

-[36] The radioisotope pollution for Iidate village from Fukushima Daiichi power plant was determined by the leak mainly on March 15, 18 and 20.

The radioisotope pollution from Fukushima Daiichi nuclear power plant was limited because the diffusion of radioisotopes was diminished by mountain , from the altitude of 500 m to 1192 m.

The difference between Fukushima Daiichi nuclear power plant and Chernobyl nuclear power plant in radioisotope pollution can be explained by the fact that the former was affected by landform more than precipitation while the latter was affected by precipitation more than the landform.

-[37]A special problem of spatial resolution which cannot be solved by fractal analysis, however, is the existence of "hot spots". Such hot spots can be very small and therefore may not be detected due to the grid distance of the monitoring stations, i. e., not because of the sparsity of the phenomenon but due to its small spatial extension. For example, in a region of relatively high mean deposition (Weinsberg Forest), with a ^{137}Cs concentration of 53 ± 14 kBq m^{-2}, the mean size of hot spots with a mean > 100 kBq m^{-2} (about twice the regional mean) has been estimated to be 440m^2 , with a mean > 150 kBq m^{-2} (about 3 times the regional mean), it is even only 2 m^2.

-[38] The model discussed in this paper indicates that multifractal techniques may be useful in estimating the ^{l37}Cs cumulative soil deposition measured in many European Countries after the Chernobyl accident.

The corresponding algorithm provides estimates of radioactive concentrations in large areas where no experimental data are available: this result is important, taking into account the low density of sampling sites.

The simulations agree well with the available measurements, and the asymptotic hyperbolic behaviour of the experimental data is well reproduced.

Thus, these results might be indicative for the possibilities of the multifractal model and be of interest for nuclear and atmospheric physicists, e.g. to fix and calibrate long range transport models, and may also provide information for epidemiological purposes and risk assessment.

In principle, it would be possible the estimation of the absorbed doses even where no data are available, and generate risk maps.

R E F E R E N C E S

[1] Mandelbrot, B. (**1982**) The Fractal Geometry of Nature. Freeman, San Francisco.

[2] Mandelbrot, B. (**1989**) Les Objets Fractals, Forme, Hasard, Dimension. 3rd Edition, Flammarion, Paris

[3] J. Theiler: Estimating fractal dimension, Vol. 7, No. 6/June **1990**/J. Opt. Soc. Am. A 1055-1073.

[4] Dubuc B, Quiniou F, Roques-Carmes C, Tricot C, Zucker SW: Evaluating the fractal dimension of profiles. Phys Rev A 39:1500–1512, **1989**.

[5] V. Cuculeanu and A. Lupu: Fractal dimensions of the outdoor radon isotopes time series. Environment International, Vol.22, Suppl. 1, pp. S171-S179, **1996**, Elsevier Science Ltd.

[6] Hurst, H.E.; Black,R.P.; Simaika, Y.M. Long-term storage: An experimental study. London: Constable; **1965**.

[7] J. Feder: Fractals. New York, NY: Plenum Press; **1988**.

[8] P. Grassberger, I. Procaccia: Characterization of strange attractors. Phys. Rev. Lett. 50, 346-349, **1983**.

[9] J.F. Gouyet: Physique et structure fractales. Paris: Masson; **1992**.

[10] M. Eisenbud: Environmental Radioactivity, Academic Press, **1973**.

[11] M. Eisenbud, T. Gesell: Environmental Radioactivity , Academic Press, **1997**.

[12] V. Cuculeanu, F. Simion, Elena Simion, A. Geicu: Dynamics, deterministic nature and correlations of outdoor ^{222}Rn and ^{220}Rn progeny concentrations measured at Bacău, Romania. Journal of Environmental Radioactivity, 102, 703-712, **2011**, Elsevier.

[13] Rapport UNSCEAR 1982, Rayonnements ionisants: sources et effets biologiques http://www.unscear.org/docs/reports/**1982**/1982-D_unscear.pdf.

[14] J. Porstendorfer: Properties and behaviour of radon and thoron and their decay products in the air, Fifth International Symposium on the Natural Radiation Environment, Commission of the European Communities, Report EUR 14411 EN, **1993**.

[15] V. Cuculeanu, S. Sonoc and M. Georgescu: Radioactivity of radon and thoron daughters in Romania, Radiation Protection Dosimetry, Vol.45, No.1/4, p.483-485, Nuclear Technology Publishing, Oxford University Press, U.K, **1992**.

[16] IAEA: Measurement and calculation of radon releases from NORM residues. International Atomic Energy Agency, Technical Report Series No. 474, Vienna, **2013**.

[17] L. Devendra, J.R. Arnold, M. Honda: Cosmic ray production rate of ^{7}Be in Oxygen, and ^{32}P, ^{33}P, ^{35}S in Argonat Mountain Altitude, Phys. Rev. 118, 1626-1632,**1960**.

[18] V.Cuculeanu, C. Dovlete, S. Sonoc, Mihaela Alexandrescu: Study on the radioactivity of the fallout during 1980-1981, Revue Roumaine de Physique, Tome 28, No. 2, 167-174, Bucharest, **1983**.

[19] G. Semenescu, S. Râpeanu, T. Magda: Fizica atomică şi nucleară. Editura tehnică, Bucureşti, **1976**.

[20] Ş. Muscalu: Fizica atomică şi nucleară. Editura didactică şi pedagocică, Bucureşti, **1976**.

[21] F.W. Sears, M.W. Zemansky, H.D.Young: Fizică. Editura didactică şi pedagocică, Bucureşti, **1983**.

[22] A. Rodna, Oana Velicu, T. Fierbântu,Victoria Plăviţu: Limitarea şi monitorizarea impactului radiologic al funcţionării unei centrale nuclearoelectrice de tip CANDU – Abordarea organismului de reglementare în domeniul nuclear din România, Forumul Regional al Energiei-FOREN 2008, Neptun, 15-19 Iunie **2008**, Cod lucrare: Sp-74-ro.

[23] http://mmediu.ro/vechi/departament_mediu/centrala_cernavoda/Fisa_U1_U2.pdf.

[24] S.N. Nuclear-electrica S.A., CNE Cernavoda: Rezultatele monitorizării factorilor de mediu şi al nivelului radioactivităţii în zona Cernavodă, Raport Informativ IR-96200-037, 26 aprilie **2012**.

[25] http://en.wikipedia.org/wiki/Windscale_fire.

[26]http://en.wikipedia.org/wiki/Three_Mile_Island_accident.

[27] Reveica Ion-Mihai: Radioactivitatea şi circuitul izotopilor radioactivi în mediu. Editura Universităţii Bucureşti, **1998**.

[28] I. Chiosilă, L. Toro, V. Cuculeanu: Radioactivitatea mediului înconjurător-Aspecte teoretice şi practice. Agenţia Naţională pentru Protecţia Mediul, Proiect MMP/**2012**, Bucureşti 2012, ISBN 978-973-0-14038-5

[29] http://en.wikipedia.org/wiki/Fukushima_Daiichi_nuclear_disaster.

[30] J. Planinc, B. Vukovic, V. Radolic, Z. Faj, D. Stanic. Deterministic chaos in radon time variations. V. simpozij HDZZ, Stubičke Toplice, 349-354, **2003**.

[31] V. Radolic, B. Vukovic, D. Stanic, J. Planinic. Radon chaotic regime in the atmosphere and soil. ISSN1330–0008, CODENFIZAE4, FIZIKA A 14 (**2005**) 2, 195–206.

[32] E.Girolleti. Fractal analysis of radon indoor time series with rescaled range and box counting methods. Proceedings of the second workshop on Radon Monitoring in Radioprotection, Environmental and/or Earth Sciences: ICTP, Trieste, Italy, 25 November- 6 December **1991**, 197-212.Edited by G.Furlan, L.Tommasino

[33] Miraç Kamişlioğlu and Fatih Külahci. Chaotic Behavior of Soil Radon Gas and Applications. Acta Geophysica, vol. 64, no. 5, Oct. 2016, pp. 1563-1592 doi: 10.1515/acgeo-**2016**-0077.

[34] Yongmei Li, Wanyu Tan, Kaixuan Tan, Zehua Liu and Yanshi Xie. Fractal and chaos analysis for dynamics of radon exhalation from uranium mill tailings. Fractals, Vol. 24, No. 3 (**2016**) 1650029 (1-8), World Scientific Publishing Company, DOI: 10.1142/ S0218348X16500298.

[35] G. Pausch, P. Bossew, W. Hofmann. Analysis of chaotic behaviour of indoor radon concentrations Conference on Radon in the Living Environment, 19-23 April 1999, Athens, Greece, 37-51

[36] Keisuke Saito, Susumu Ogawa: Fractal dimensions for radioisotope pollution patterns by nuclear power plant accidents. The International Archives of the Photogrammetry, Remote Sensing and Spatial Information Sciences, Volume XL-7/W3, 2015. 36th International Symposium on Remote Sensing of Environment, 11–15 May **2015**, Berlin, Germany.

[37] G. Pausch, P. Bossew, W. Hofmann, F. Steger Multifractal analysis of the ^{137}Cs-fallout pattern in Austria resulting from the Chernobyl accident. IRPA Regional Symposium: Radiation Protection in Neighbouring Countries of Central Europe. Prague, 8-12 September **1997**.

[38] G. Salvadorit, S.P. Ratti, G. Belli Modelling the Chernobyl radioactive fallout(II): A multifractal approach in some european countries *Chemosphere*, Vol. 33, No. 12. pp. 2359-2311, **1996**, Elsevier Science Ltd.

[39] Sprott, J.C., **2003**. Chaos and Time-Series Analysis, Oxford University Press Inc., New York.